

# A Semi-Empirical Equation based on the Strut-and-Tie Model for the Shear Strength Prediction of Deep Beams with Multiple Large Web Openings

Lara T. Hussein

Department of Civil Engineering  
College of Engineering  
University of Baghdad  
Baghdad, Iraq  
l.hussein1001@coeng.uobaghdad.edu.iq

Rafaa M. Abbas

Department of Civil Engineering  
College of Engineering  
University of Baghdad  
Baghdad, Iraq  
dr.rafaa@coeng.uobaghdad.edu.iq

Received: 9 January 2022 | Revised: 25 January 2022 | Accepted: 27 January 2022

**Abstract**—The behavior and shear strength of full-scale (T-section) reinforced concrete deep beams, designed according to the strut-and-tie approach of ACI Code-19 specifications, with various large web openings were investigated in this paper. A total of 7 deep beam specimens with identical shear span-to-depth ratios have been tested under mid-span concentrated load applied monotonically until beam failure. The main variables studied were the effects of width and depth of the web openings on deep beam performance. Experimental data results were calibrated with the strut-and-tie approach, adopted by ACI 318-19 code for the design of deep beams. The provided strut-and-tie design model in ACI 318-19 code provision was assessed and found to be unsatisfactory for deep beams with large web openings. A simplified empirical equation to estimate the shear strength for deep T-beams with large web openings based on the strut-and-tie model was proposed and verified with numerical analysis. The numerical study considered three-dimensional finite element models, in ABAQUS software, that have been developed to simulate and predict the performance of deep beams. The results of numerical simulations were in good agreement and exhibited close correlation with the experimental data. The test results showed that the enlargement in the size of web openings substantially reduces the elements' shear capacity. The experiments revealed that increasing the width of the openings has more effect than the depth at reducing the load-carrying capacity.

**Keywords**—deep beams; reinforced concrete; T-beams, web opening; strut-and-tie model; finite element analysis; shear strength

## I. INTRODUCTION

Shear behavior of reinforced concrete members (slender members that have span-to-depth ratios greater than 2.5) is a complex phenomenon which is influenced by a large number of parameters [1, 2]. This complexity is more pronounced in deep beams (members that have small, less than 2.5, span-to-depth ratios) because the applied load is transferred mainly through the formation of arching which causes a highly nonlinear strain distribution in the cross section so that the shear strain is

dominant [3, 4]. In deep beams, the strain distribution is nonlinear and the load is transferred to the support by a compression strut joining the loading point and the support [2, 5-9]. The creation of web openings is often required for the accommodation of electrical and mechanical conduits. Enlargement of openings due to architectural/mechanical requirements may reduce the element's shear capacity [9, 10]. Design code provisions typically use sectional models to determine the shear and flexure capacities of slender members [11-13]. In deep beams, traditional sectional design approaches based on plane sectional theory are not applicable, a nonlinear distribution of strains dominates the response and arch action becomes the primary force-transfer mechanism following diagonal cracking [5, 13]. Most codes of practice rely on empirical or semi-empirical equations for the design of deep beams, however, these equations are limited by the extent of the experimental results used for their calibration [2]. Modern design codes such as EC2 and ACI 318-19 have adopted design approaches based on the implementation of Strut-and-Tie mechanistic Models (STMs) because they appear more rational and relatively simple to apply. The design of deep beams based on the strut-and-tie model relies on the lower bound theory of plasticity and assumes that both concrete and steel are perfectly plastic materials [3]. The STM idealizes the complex flow of stresses using a pin-jointed truss consisting of compression struts and tension ties, which allows easier monitoring of the force flow [14]. There is no provision for the designing of deep beams with openings in current design codes.

In the current study, 7 deep beams were tested until failure and a comparison was made with the strut-and-tie design approach adopted by the ACI 318-19 code. The effects of the openings were also considered. From the experimental results, it can be noticed that increasing the width of the openings has more effects than increasing the depth in reducing the load carrying capacity. This agrees with the statement that as the opening's distance from what can be called the loaded quadrant to the unloaded quadrant, the strength of the beam increases [15]. The experimental results were compared with the

Corresponding author: Lara T. Hussein

numerical finite element analysis results of [16]. Opening's configuration was investigated in [17, 18] and an increase in ultimate load capacity compared with that of quadrilateral openings when circular openings were used was reported in [19].

Finite Element Modeling (FEM) is one of the most powerful tools in simulating structural elements in a variety of fields. The successful simulation of specific elements relies upon the realistic representation of the material properties in FEM. However, due to the complexity of the constitutive material properties concrete, modeling the behavior of reinforced concrete, in particular shear, has been, and still is, a challenging issue [16, 20].

## II. STRUT-AND-TIE MODEL

The STM is based on the fact that within a distance from a source of disturbance such as a concentrated load or support, the distribution of strain in the member is nonlinear (St. Venant's principle) [10, 21]. Plain sections do not remain plain. Nonlinear strain distributions in concrete members, caused by changes in geometry or loading conditions, are referred to as a disturbed regions or D-regions [14] (D-for discontinuity or disturbed), while, the linear strain distribution regions are called B-regions (B-for Bernoulli or beam). The STM is an approach to design discontinuous D-regions in reinforced concrete structures to reduce the complex states of stress into a truss comprised of simple, uniaxial stress paths [21] (Figure 1).

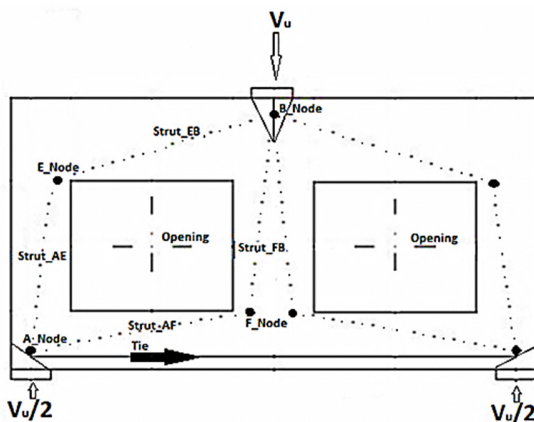


Fig. 1. Strut-and-tie formation in deep beam, truss model (strut, tie, and nodes).

These truss models represent all internal force effects and do not require separate flexure and shear models, as in the slender member case. Strut-and tie modeling is based on the lower-bound theory of plasticity and the model capacity is always less than the actual capacity [14]. Struts are used to represent the assumed compressive stress fields in the concrete. Ties represent the primary tension reinforcement with the tie location made to correspond to the centroid of the reinforcement. While the tie also consists of the concrete surrounding the reinforcement, this concrete is not directly considered in the design but will reduce the tie elongation [22]. The struts and ties intersect at nodes. Most design specifications recognize 3 major node types: CCC-nodes

bounded by struts only, CCT-nodes bounded by one tie and two or more struts, and CTT-nodes bounded by one strut and two or more ties. The ACI design provision allows the use of any truss configuration according to the designer provisions [2, 21].

## III. EXPERIMENTAL WORK

Seven full scale reinforced concrete deep beams with large web openings were casted and tested until failure in order to study their shear strength. The objectives of this study were to investigate experimentally the main parameters of the laboratory testing which include:

- The width of the opening  $E$ , considering  $E/L$  as the ratio of the width of the opening to the shear span of the beam as: 0.4, 0.53, 0.67.
- The depth of opening  $D$ , adopting  $D/H$  as the ratio of depth of the opening to the height of the beam section as: 0.48, 0.6.

The constants were:

- Concrete compressive strength.
- Type of loading.
- Span length to height of the section ratio ( $L/H$ ).
- The two openings were symmetrically located relative to the center-line of the beam and the center of each opening was located at  $0.45H$  from the soffit of the beam.

The experimental specimens were designed according to ACI 318-19 and were fabricated with dimensions of 1950mm length, 1000mm height, 750mm flange width, 125mm flange thickness, and 250mm web thickness. The testing program of this study tried to investigate deep beams with large web openings, with varying  $E/L$  ratio (0.4, 0.53, 0.67), and  $D/H$  ratio (0.48, 0.6), designated by [DP-DE], where DP stands for Deep Beam, D for the opening depth, and E for the opening width. The symbols for the reinforced deep beams with large web openings and for the solid beam were DP\_48x36, DP\_48x48, DP\_48x60, DP\_60x36, DP\_60x48, DP\_60x60, and DP\_solid that was subjected to static loading.

### A. Concrete Materials

For concrete production, the cement, sand, coarse aggregate mixing ratio was 1: 1.7: 2.6 in weight. The water-cement ratio was 0.5 for the production of ordinary concrete with compressive strength of 25MPa.

### B. Steel Reinforcement

For all specimens, the longitudinal deformed steel bars that have been used in this study had nominal diameter of 16mm and 10mm for the main reinforcement and the compression reinforcement respectively. For shear reinforcements and skin reinforcements, steel bars of 8mm diameter were used. Reinforcement diameters and spacing were chosen according to the ACI318-19 requirements. According to ASTM A615, tensile tests for the steel bars were carried out using the testing machine available in the Laboratory of Construction Materials at the College of Engineering, University of Baghdad. All deep

beams had the same distribution-ratio of interior steel reinforcement. The main (longitudinal flexural tensile) reinforcement is 3  $\varnothing$  16mm deformed steel bars, while the longitudinal compression reinforcement is 4  $\varnothing$  10mm deformed steel bars. The proposed flexural tension reinforcement aspect has been checked with Articles 9.9.3.2 and 9.6.1 of the ACI

318M, 2019. Skin reinforcement and vertical shear reinforcement (stirrups) were designed and distributed with  $\varnothing$  8mm@150mm along the 2-sides. Proposed stirrups reinforcement aspects have been checked with Articles 9.9.3.1 and 9.9.4.3 of the ACI 318M, 2019 (Figure 2).

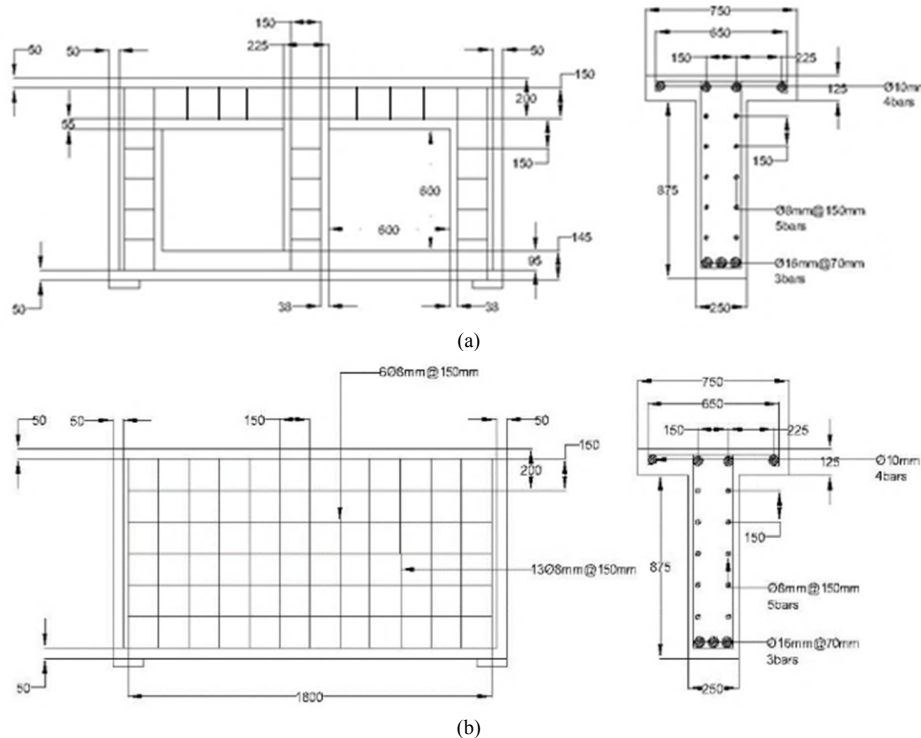


Fig. 2. (a) Steel reinforcement in the experimental work of DP-60x60. (b) Steel reinforcement in the experimental work of DP-Solid.

### C. Test Setup

Upon the completion of the preparation, installation, and calibration of all devices and equipment required for the tests (Figure 3), the beams were subjected to monotonically increasing static loading up to failure.



Fig. 3. Equipment and test setup.

The experimental investigation was carried out using a 500kN capacity hydraulic actuator that exposed the structural member to a concentrated load that was applied in 5kN increments. The tested specimens were simply supported and bearing plates under the load and above the supports have been used to better distribute the stress and to avoid any local crushing.

## IV. EXPERIMENTAL TEST RESULTS

### A. Load-Deflection Relations

At each load step of the static test program, the vertical deflection of the specimens was recorded and the following conclusions were drawn:

- For an increase of the opening width from 360mm to 600mm, and of the E/L from 0.4 to 0.67, the load carrying capacity of the beams was reduced by about 66%, for Group- 60 and Group- 48 [10] (Figure 4).
- Increase in the opening depth from 480mm to 600mm, and in D/H from 0.48 to 0.6, led to a reduction in the load carrying capacity of about 25% (Figure 4).
- For Group- 48 and Group- 60, the load-deflection relations behave more as a linear relation because of the reduced

beam rigidity, EI, as a result of introducing large web openings [23].

- Group- 60 has less load carrying capacity than Group-48 as a result on increasing opening depth that led to beam stiffness reduction [15].
- Increased deflection was noticed at increasing opening width as a result of reduced rigidity, EI, and hence, increased displacements [9].
- Figure 4(c) shows the significant effect of opening presence in reducing load carrying capacity, introducing web openings of E-600mm x D-600mm which can reduce the load carrying capacity by about 300% as compared with the solid beam, resulting to reduced rigidity and increased displacement.
- As the opening enlarged, the deep beams were exposed to higher stresses as a result of opposing the web opening to the compression struts and intersecting the load path propagation which in turn reduced the deep beam capacity [3].
- Increasing the opening width has more effect in decreasing the load carrying capacity of the deep beams than increasing its depth. The more opposed the opening sites in the inner quarter of the shear span to the load path that propagates from the support to the applied load region, the more reduction in the load carrying capacity.

#### B. Crack Pattern, Load Capacity, and Failure Mode

During each test, cracks were marked at each discrete load increment. Figure 5 shows typical crack patterns of the 7 specimens. Specimens with web openings were having the same response and behavior up to failure. A summary of first crack load, flexure cracks, ultimate load, and failure mode is presented in Figure 5(a) which shows the crack pattern for DP\_48x48. A crack pattern comparison of the experimental and the finite element analysis results can be seen in Figure 5(b).

The crack pattern at each load increment was marked. The first inclined crack was propagating from the support regions toward the lower opening corner at load 20-30% of the ultimate load as shown in Figure 5(a) with the crack designated with number (1) being the first crack. At load 25-35% of the ultimate load, a diagonal tension crack number (2) propagated at the upper opening corner toward the applied load region. Flexural number (3) cracks appeared at 35-44% of the ultimate load. A typical cracking pattern (beam-column) conjunction, horizontal crack, appeared at loading stage 44-50% of the ultimate load as indicated by crack numbering (4). At loading stage 40-60% of the ultimate load, the tension cracks designated with number (2) propagated in the flange with additional inclined crack approaching near the applied load region appeared (crack number (5)). The serviceability load, i.e. a diagonal crack reaching width of 0.3mm appeared at 60% of the ultimate load. At increasing load until failure, cracks that start at the support regions extend toward the opening corner cracks and fuse with them forming long cracks that got wider until the beam failed. The shear failure is indicated with

number (6). The crack patterns shown in Figure 5(a) present the strut-and-tie formation as expected for the load-path. The stress path and strut-and-tie configurations are shown clearly in Figures 5(a)-(b) [10].

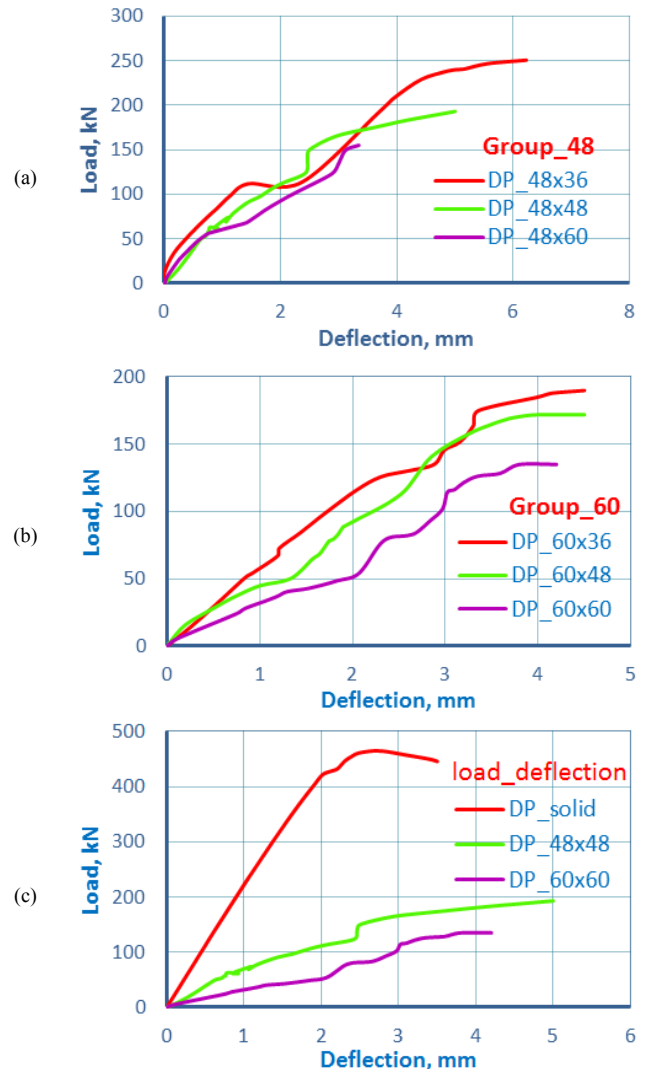


Fig. 4. Comparison of load-deflection curves for DP\_48 group and DP\_60 group with solid case. (a) load-deflection curve of Group\_48, (b) load-deflection curve of DP\_60 group, (c) load-deflection curve of DP-48x48, DP-60x60, and DP-Solid.

Introducing large web openings in the deep beam transforms it into an ordinary connected beam-column (crack number (4)) [10]. The load-deflection curve behaves semi-linearly, which proves that the deep beams act as ordinary beams more than as deep beams, as a result of the larger web openings at the shear zone which change their geometry (Figure 6) [23]. Introducing web openings intersects the stress path and leads to changed deep beam geometry which affects the deep beam behavior and shear capacity [23]. The tested specimen DP\_48x48 as obtained from ABAQUS program is shown in Figure 5(b). The crack patterns were selected at the failure stage. The initial cracks were generated at the support regions and propagated

toward the lower corner of the openings. Cracks at the upper corner of the opening extended toward the applied load region, which is compatible with the experimental tests. This comparison showed complete matching with the experimental results.

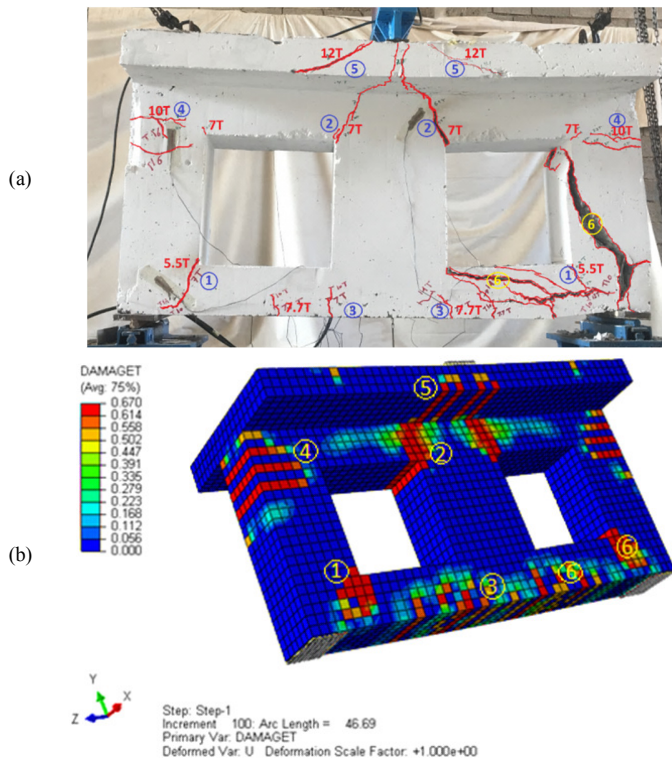


Fig. 5. (a) Designated experimental crack pattern of DP\_48x48, and T- for TON, (b) Designated crack pattern of the numerical finite element model for specimen DP\_48x48.

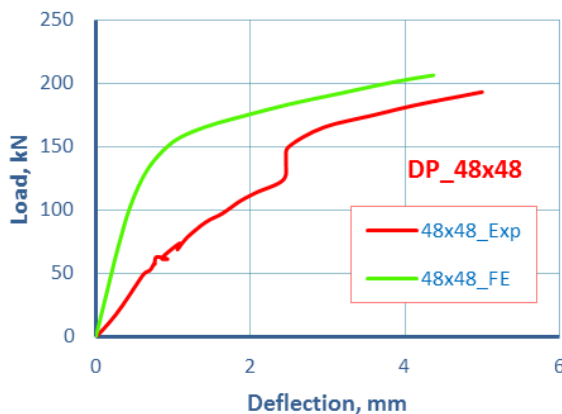


Fig. 6. Comparison of experimental and finite element load-deflection relations of specimen DP\_48x48.

V. THE PROPOSED EMPIRICAL EQUATION

In ACI design code there is no provision for designing deep beams with web openings. The STM provided by ACI code overestimates the actual strength of the deep beams with web openings, while it is based on the lower bound theorem, adding

a numerous error in the design based on ACI approach. For this reason, in this study, 7 deep beams were tested and the results were compared with the numerical finite element results implemented in Abaqus in order to investigate the opening effects on the load carrying capacity of the deep beams. The specimens shear strength is specimen-size dependent, it increases when size increase:

$$\frac{V_{u)solid}}{HL} = \frac{V_{u)opening}}{ED} \quad (1)$$

where  $V_{u)solid}$  is the load-carrying capacity, ultimate shear strength in deep beam without web opening,  $V_{u)opening}$  is the opening imaginary shear capacity, H is the depth of the beam, L it's the shear span, E the opening width, and D the opening depth. From (1), we get:

$$V_{u)opening} = \frac{ED}{HL} \cdot V_{u)solid} \quad (2)$$

The shear strength for deep beam with opening  $V_{u)ODP}$ :

$$V_{u)ODP} = V_{u)solid} - V_{u)opening}$$

$$V_{u)ODP} = \left(1 - \frac{ED}{HL}\right) \cdot V_{u)solid} \quad (3)$$

Then, by comparing the tests results of 66 specimens modeled with Abaqus, with a wide range variety of opening depths and widths from 100mm to 800mm, and by trial and error procedure, the empirical equation was created. The results showed that the opening width has more effect than the opening depth on decreasing the ultimate capacity. Also, the load carrying capacity of the deep beam decreases as the ratio of the web opening size to shear span-to-depth of deep beam increases accordingly to the proposed equation. The inclusion of web opening width to the shear span ratio, which is the most influential factor on the shear behavior of the deep beam, into the proposed equation gives us:

$$V_{u)ODP} = \left(1 - \frac{ED}{HL}\right) / \left(1 + \frac{E}{L}\right) \cdot V_{u)solid} \quad (4)$$

$$V_{u)Pstm} = \left(1 - \frac{ED}{HL}\right) / \left(1 + \frac{E}{L}\right) \cdot V_{u)stm}$$

where:  $V_{u)solid} = V_{u)stm}$  and  $V_{u)ODP} = V_{u)Pstm}$ .

The applicability of this equation is limited to deep beams with shear span to depth ratio of 0.95. The center of the openings is located at 0.45H from the soffit of the beam and the opening location at the inner quarter of the shear span. Regression analysis was conducted for the theoretical results and the effects of depth, width, and opening size to shear span to beam depth ratio on the shear strength of the beam and the results are shown in Figure 7.

VI. FAILURE LOAD

The calibration of the failure load obtained from the finite element analysis, the experimental work, and the proposed equation for deep beams with web openings in strut-and-time approach for each static tested specimen is shown in Table I. In the finite element analysis, the failure load is defined as the solution for a minimum increment of load that does not converge due to numerous cracks. Abaqus overestimates the failure load of the specimens since the finite element method

considers the modeled member as rigid bodies which show stiffer and stringer behavior than the real ones. The higher stiffness in the finite element models come from several factors adopted in the finite element analysis. A perfect bond is assumed between the steel bars and the concrete. In reality, there is a slip percentage that reduces the composite action between the steel bars and concrete [24]. Also, the finite element analysis ignores the micro crack effects that exist due to the drying shrinkage of the concrete that reduces the stiffness of the actual specimens. Thus, the overall stiffness of the finite element models is higher than that of the experimental ones.

TABLE I. COMPARISON OF THE FAILURE LOAD FOR THE EXPERIMENTAL, STM, AND FEM BEAMS

Specimen	Failure load, KN			$\frac{V_{pstm}}{V_{uEXP}}$	$\frac{V_{uFEM}}{V_{uEXP}}$
	$V_{uEXP}$	$V_{upstm}$	$V_{uFEM}$		
DP-48x36	260	226	280	0.86	1.07
DP-48x48	200	189	210	0.94	1.05
DP-48x60	156	157	170	1.00	1.08
DP-60x36	210	201	230	0.95	1.09
DP-60x48	172	150	180	0.87	1.04
DP-60x60	135	120	150	0.89	1.11
DP-Solid	495	400	546	0.80	1.10

VII. CONCLUSION

In this paper, seven full scale deep beams with different web openings were examined. The main variables studied were the effects of width and depth of the web openings on the performance of the deep beams. The following conclusions can be drawn from the findings of this study:

- From the experimental results it can be noticed that increasing the width of the opening has more pronounced effect than the opening depth at reducing the load carrying capacity.
- Increasing the opening width (i.e. increasing the E/L ratio from 0.4 to 0.67) reduces the load carrying capacity by about 50%, while increasing the opening depth (i.e. increasing D/H ratio from 0.48 to 0.6) led to a reduction in the load carrying capacity by about 28%.
- The first visible inclined cracks normally appeared in the support bearing regions and formed toward the opening corner at load levels of about 20-30% of the ultimate load.
- The calibrated numerical models indicated that load deflection response was stiffer than the experimental one and there was a good agreement in both trend and amplitude with variation in the load capacity by about 5% to 10%.
- The strut-and-tie approach for the design based on ACI 318-19 code provisions may over predict the shear strength of the deep T-beam with large opening up to about 125% of the actual capacity because it ignores the web opening effects.
- The proposed empirical equation, based on the STM of the ACI code, showed good agreement with the experimental and numerical results of about 90%.

The study recommends investigating the limits of the critical web opening size that turn the nonlinear behavior of deep beams into linear.

ACKNOWLEDGMENT

The authors would like to express their gratitude to the staff of the Civil Engineering Department at the University of Baghdad.

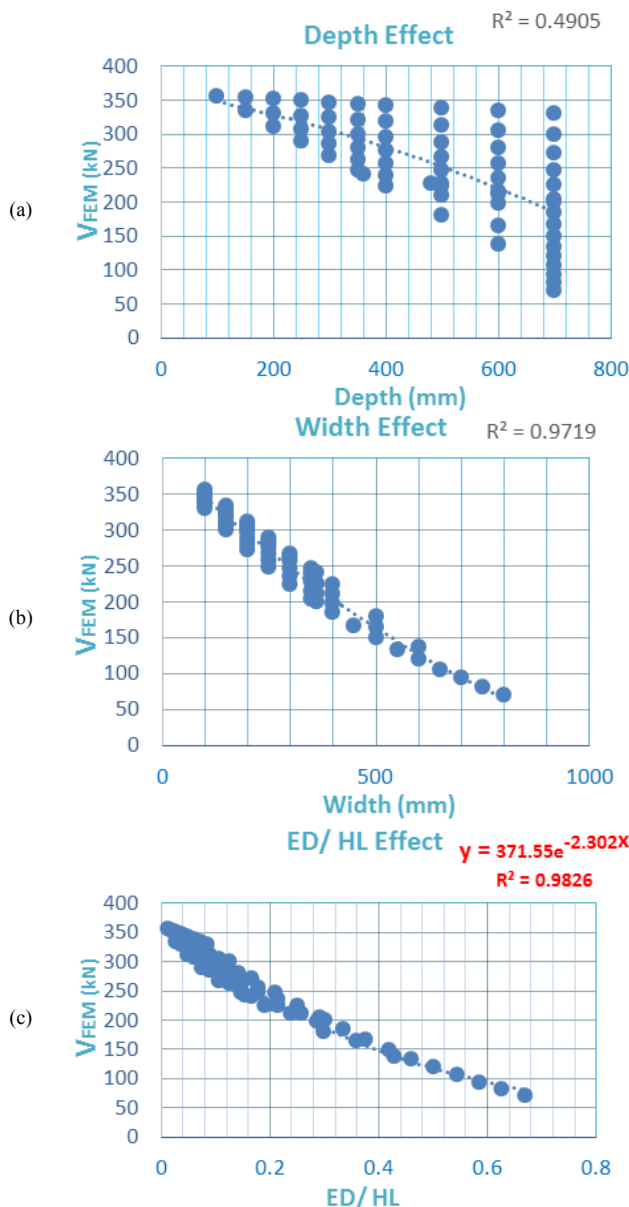


Fig. 7. Opening (a) depth, (b) width, and (c) size to shear span to depth ratio effect on deep beams.

## REFERENCES

- [1] K. H. Tan and H. Y. Lu, "Shear Behavior of Large Reinforced Concrete Deep Beams and Code Comparisons," *Structural Journal*, vol. 96, no. 5, pp. 836–846, Sep. 1999, <https://doi.org/10.14359/738>.
- [2] M. P. Collins, E. C. Bentz, and E. G. Sherwood, "Where is Shear Reinforcement Required? Review of Research Results and Design Procedures," *Structural Journal*, vol. 105, no. 5, pp. 590–600, Sep. 2008, <https://doi.org/10.14359/19942>.
- [3] K. S. Ismail, M. Guadagnini, and K. Pilakoutas, "Strut-and-Tie Modeling of Reinforced Concrete Deep Beams," *Journal of Structural Engineering*, vol. 144, no. 2, Feb. 2018, Art. no. 04017216, [https://doi.org/10.1061/\(ASCE\)ST.1943-541X.0001974](https://doi.org/10.1061/(ASCE)ST.1943-541X.0001974).
- [4] L. D. Lorenzis and A. Nanni, "Shear Strengthening of Reinforced Concrete Beams with Near-Surface Mounted Fiber-Reinforced Polymer Rods," *Structural Journal*, vol. 98, no. 1, pp. 60–68, Jan. 2001, <https://doi.org/10.14359/10147>.
- [5] G. Zhang *et al.*, "Reinforced concrete deep beam shear strength capacity modelling using an integrative bio-inspired algorithm with an artificial intelligence model," *Engineering with Computers*, Dec. 2020, <https://doi.org/10.1007/s00366-020-01137-1>.
- [6] J. Wight, *Reinforced Concrete: Mechanics and Design*, 3rd ed. Upper Saddle River, NJ, USA: Prentice Hall, 1997.
- [7] S. T. Mau and T. S. T. C. Hsu, "Formula for the Shear Strength of Deep Beams," *Structural Journal*, vol. 86, no. 5, pp. 516–523, Sep. 1989, <https://doi.org/10.14359/3008>.
- [8] K. N. Smith and A. S. Vantsiotis, "Shear Strength of Deep Beams," *Journal Proceedings*, vol. 79, no. 3, pp. 201–213, May 1982, <https://doi.org/10.14359/10899>.
- [9] W. A. Jasim, Y. B. A. Tahnat, and A. M. Halahla, "Behavior of reinforced concrete deep beam with web openings strengthened with (CFRP) sheet," *Structures*, vol. 26, pp. 785–800, May 2020, <https://doi.org/10.1016/j.istruc.2020.05.003>.
- [10] O. E. Hu and K. H. Tan, "Large reinforced-concrete deep beams with web openings: test and strut-and-tie results," *Magazine of Concrete Research*, vol. 59, no. 6, pp. 423–434, May 2007, <https://doi.org/10.1680/macr.2007.59.6.423>.
- [11] D. B. Birrcher, "Design of reinforced concrete deep beams for strength and serviceability," Ph.D. dissertation, University of Texas at Austin, Austin TX, USA, 2009.
- [12] ACI-ASCE Committee 445, *445R-99: Recent Approaches to Shear Design of Structural Concrete (Reapproved 2009)*. ACI, 2009.
- [13] M. F. Andermatt and A. S. Lubell, "Behavior of Concrete Deep Beams Reinforced with Internal Fiber-Reinforced Polymer—Experimental Study," *Structural Journal*, vol. 110, no. 4, pp. 585–594, Jul. 2013, <https://doi.org/10.14359/51685744>.
- [14] J. Schlaich, K. Schafer, and M. Jennewein, "Toward a Consistent Design of Structural Concrete," *PCI Journal*, vol. 32, no. 3, pp. 74–150, May 1987, <https://doi.org/10.15554/pci.05011987.74.150>.
- [15] S. P. Ray and C. S. Reddy, "Strength of reinforced deep beams with and without opening in the web," *The Indian Concrete Journal*, vol. 53, no. 9, pp. 242–246, Sep. 1987.
- [16] A. Y. Pranata, D. Tjitradi, and I. Prasetya, "Horizontal Web Reinforcement Configuration Analysis of Deep Beam Capacity and Behavior using Finite Element Modeling," *Engineering, Technology & Applied Science Research*, vol. 10, no. 1, pp. 5242–5246, Feb. 2020, <https://doi.org/10.48084/etasr.3256>.
- [17] M. A. J. Hassan and A. F. Izzet, "Serviceability of Reinforced Concrete Gable Roof Beams with Openings under Static Loads," *Engineering, Technology & Applied Science Research*, vol. 9, no. 5, pp. 4813–4817, Oct. 2019, <https://doi.org/10.48084/etasr.3110>.
- [18] N. H. Saksena and P. G. Patel, "Effects of the circular openings on the behavior of concrete beams without additional reinforcement in opening region using fem method," *International Journal of Advanced Engineering Technology*, vol. 4, no. 2, 2013.
- [19] A. Shubbar, H. Alwan, E. Y. Phur, J. McLoughlin, and A. Al-khaykan, "Studying the Structural Behaviour of RC Beams with Circular Openings of Different Sizes and Locations Using FE Method," *International Journal of Structural and Construction Engineering*, vol. 11, no. 7, pp. 916–919, 2017.
- [20] M. A. J. Hassan and A. F. Izzet, "Experimental and Numerical Comparison of Reinforced Concrete Gable Roof Beams with Openings of Different Configurations," *Engineering, Technology & Applied Science Research*, vol. 9, no. 6, pp. 5066–5073, Dec. 2019, <https://doi.org/10.48084/etasr.3188>.
- [21] K. Mohamed, A. S. Farghaly, and B. Benmokrane, "Strut Efficiency-Based Design for Concrete Deep Beams Reinforced with Fiber-Reinforced Polymer Bars," *Structural Journal*, vol. 113, no. 4, pp. 791–800, Jul. 2016, <https://doi.org/10.14359/51688476>.
- [22] ACI-ASCE Committee 318, *ACI CODE-318-19: Building Code Requirements for Structural Concrete and Commentary*. ACI, 2019.
- [23] N. Rezaei, G. Klein, and D. B. Garber, "Effect of Development and Geometry on Behavior of Concrete Deep Beams," *Structural Journal*, vol. 116, no. 3, pp. 171–181, May 2019, <https://doi.org/10.14359/51713308>.
- [24] "Abaqus Analysis User's Guide (6.14)." <http://130.149.89.49:2080/v6.14/books/usb/default.htm> (accessed Feb. 08, 2022).